Computational Materials Science 231 (2024) 112548

Contents lists available at ScienceDirect

Computational Materials Science

journal homepage: www.elsevier.com/locate/commatsci

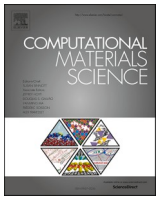

Full Length Article

Prediction of carbon nanotubes reinforced interphase properties in fuzzy fibre reinforced polymer via inverse analysis and optimisation

Marzena Pawlik [a], Huirong Le [b], Paul Wood [c], Yiling Lu [a,*]

[a] School of Computing and Engineering, College of Science and Engineering, University of Derby, Markeaton Street, Derby, DE22 3AW, UK
[b] The Future Lab, Tsinghua University, Beijing, China
[c] Institute for Innovation in Sustainable Engineering, University of Derby, Quaker Way, Derby, DE1 3HD, UK

ARTICLE INFO

Keywords:
Fuzzy fibre reinforced polymer
Nano-reinforced interphase
Inverse problem
Parameters' identification
Optimisation algorithm

ABSTRACT

This paper presents the parameter identification procedure of carbon nanotubes (CNTs) reinforced interphase in fuzzy fibre reinforced polymer (FFRP). The procedure was completed with ANSYS Workbench 19.2 software by combining Mechanical ADPL and Goal-Driven Optimisation. Firstly, a three-phase representative volume element (RVE) containing carbon fibre, CNTs reinforced interphase and epoxy resin was developed as a collection of Mechanical APDL commands. This RVE model was simulated to evaluate the elastic constants of FFRP lamina. CNTs reinforced interphase was characterised by transversely isotropic model. Interphase properties were parametrised and became input parameters in the Goal-Driven Optimisation. FFRP lamina elastic constants were set as the output parameters. Multi-objective Genetic Algorithm (MOGA) was used to identify the interphase properties, so that the output FFRP lamina elastic constants match the objective and constraints. The optimisation algorithm converged after 585 evaluations. Five potential candidate point, which met required objectives and constraints, were found. The identified interphase properties agreed well with the literature (an average percentage error of around 2%). This inverse procedure shows the potential to identify the interphase properties in nano-engineered composites, which are extremely difficult to measure experimentally.

1. Introduction

Nano-engineered fibre reinforced polymers (FRP) have received considerable attention in the composite field due to their enhanced mechanical and electrical properties. Nanofillers such as carbon nanotubes (CNTs) or graphene can be introduced to the FRP by growing on the fibre surface, forming so-called hierarchical fibres [1–5]. One of the typical examples is a fuzzy fibre with CNTs radially grown on the fibre surface, as shown in Fig. 1. Fuzzy fibres are subsequently embedded in polymeric matrix, making fuzzy fibre reinforced polymer (FFRP). The multifunctional CNTs reinforced interphase between fibres and matrix is formed. CNTs strengthen the interphase and improve properties of FFRP, including interfacial shear strength [6], flexural strength [7], transverse elastic modulus [5], thermal conductivity [8].

In the past years, researchers have focused on developing mathematical models to predict the mechanical elastic properties of these nano-engineering materials [5,9–15]. For example, Kundalwal and Ray [10,12] studied the effects of CNTs waviness on the elastic behaviour of the FFRP using analytical micromechanics based on the representative volume element (RVE) and finite element method. Chatzigeorgiou et al. [13] proposed an extension of the composite cylinders method which computed the effective properties of FFRP various CNTs volume fractions and lengths. Rao et al. [14] developed a multi-scale procedure taking into account two-scale interphase effects on the overall properties of FFRPs, including CNTs/matrix interphase and fuzzy fibre interphase. In general, these studies summarised that the out-of-plane properties of the FFRP can be significantly improved due to the unique orientation and exceptional high axial modulus of CNTs [5,13] but are greatly dependent on the CNTs volume fraction [13], CNTs radius, length and waviness [14].

Aforementioned mathematical models were forward analyses based on each constituent of FFRP, including CNTs, fibre and matrix. However, some parameters are not readily available, i.e., CNTs volume fraction in the interphase. Experimental characterisation of the interphase region remains challenging. It is commonly accepted that the interphase properties of FRPs are somewhere between fibre and matrix [18]. Interphase modulus can be measured by nanoindentation, AFM or dynamic mechanical mapping [19,20]. However, these experimental

* Corresponding author.
E-mail address: y.lu@derby.ac.uk (Y. Lu).

https://doi.org/10.1016/j.commatsci.2023.112548
Received 18 May 2023; Received in revised form 25 September 2023; Accepted 1 October 2023
Available online 12 October 2023

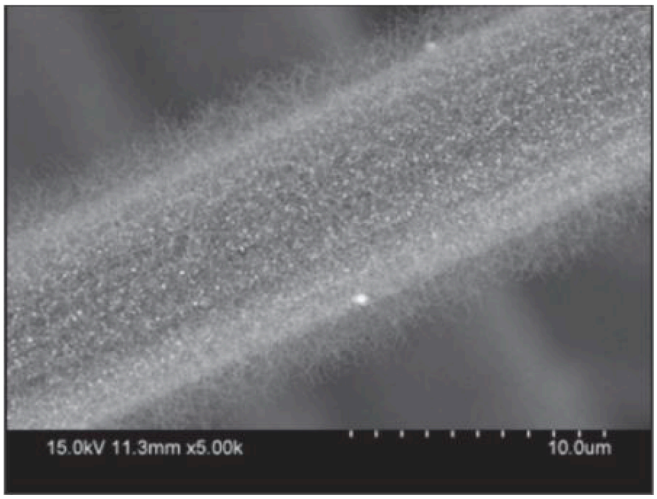

Fig. 1. A single fuzzy fibre with aligned CNTs [21].

measurement processes are very difficult to conduct due to the surface roughness, size-scale effects and tip blunting [21]. So far, there are no direct experimental measurements of the FFRP's interphase properties.

The inverse procedure is an alternative way to forward analysis that can predict the CNTs interphase properties based on the combination of optimisation algorithms with available experimental data. This technique has been successful in determining the interphase properties in nanocomposites [16] and in FRP [17,18]. For instance, Lu et al. [17] predicted stiffness of interphase region based on the experimental results, microstructural modelling method and Kriging metamodel. Matzenmiller and Gerlach [19] estimated the elastic properties of glass fibre/epoxy interphase using the generalised method of cells with the aid of a gradient-based solution algorithm. Rafiee and Ghorbanhosseini [20] developed a stochastic multi-scale model to predict mechanical properties of FFRP with randomly orientated CNTs on the fibre surface. A fuzzy fibre was viewed as two distinct phases: a core fibre and the surrounding polymer with randomly orientated CNTs. The volume fraction and waviness of CNTs were considered random variables; a good agreement between the theoretical predictions and experimental data was achieved.

In contrast to Rafiee and Ghorbanhosseini work [20], this paper presents an inverse method to predict the properties of radially grown CNTs on the fibre surface. Due to the unique orientation of CNTs, the interphase's mechanical properties in FFRP become direction-dependent. The number of predicted parameters increases, compared to the isotropic interphase (random CNTs orientation), and complicates the inverse solution. This paper presents a procedure to determine CNTs reinforced interphase properties from the RVE and known lamina properties. The optimisation process was entirely performed using FEM software package, namely ANSYS. The RVE model was simulated using ANSYS Design Parametric Language (APDL). The RVE model contained

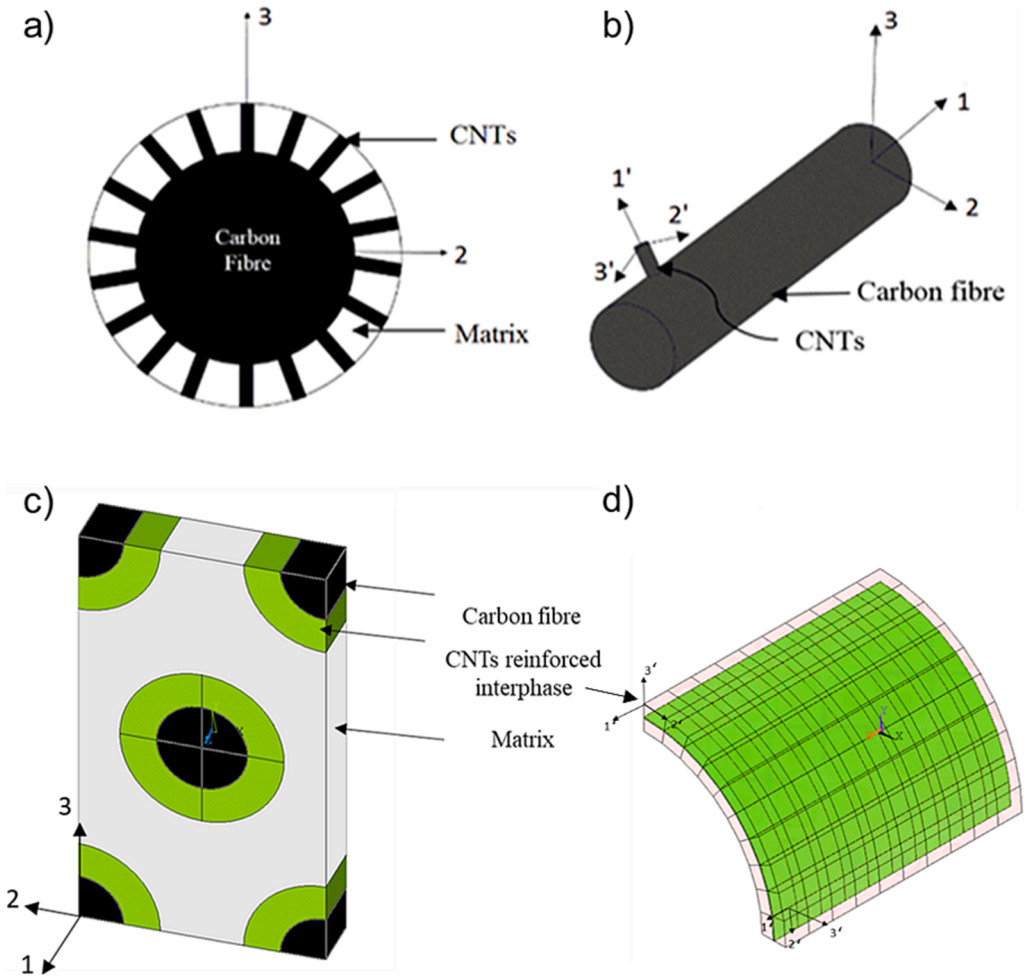

Fig. 2. Schematic illustrations of (a) Cross-section view of the fuzzy fibre, (b) Perspective view of the fuzzy fibre, (c) Hexagonal RVE model of FFRP, (d) VEORIENT command applied to the transversely isotropic interphase. 1–2-3 corresponds to a global coordinate system, where 1 is the carbon fibre longitudinal direction. Local coordinate system, 1′-2′-3′ was introduced for CNTs reinforced interphase, where 1′ is the CNTs direction.

Table 1
Mechanical properties of carbon fibre (T650), epoxy resin (Epon 862) and CNTs reinforced interphase .

Carbon Fibre (T650)		Epoxy Resin (Epon 862)		CNTs reinforced interphase	
Longitudinal modulus, E_1^f (GPa)	241.00	Modulus, E^m (GPa)	3.00	Longitudinal modulus,$E_{1'}^i$	298.64 GPa
Transverse modulus, E_2^f (GPa)	14.50	Poisson's ratio,ν^m	0.30	Transverse modulus, $E_{2'}^i$	7.01 GPa
In-plane shear modulus, G_{12}^f (GPa)	22.8			In-plane shear modulus,$G_{1'2'}^i$	2.81 GPa
Transverse shear modulus, G_{23}^f (GPa)	4.80			Transverse shear modulus,$G_{2'3'}^i$	2.52 GPa
Longitudinal Poisson's ratio ν_{12}^f	0.27			In-plane Poisson's ratio, $\nu_{1'2'}^i$ [a]	0.1
Transverse Poisson's ratio ν_{23}^f	0.51			Out-of-plane Poisson's ratio, $\nu_{2'3'}^i$ [a]	0.39
Diameter (μm)	5.00			Thickness (μm)	2.00

[a] estimated properties

adapted from [13]

three phases, including carbon fibre, CNTs reinforced interphase and epoxy resin. The FFRP material selection was motivated by the published experimental and numerical results [13]. The RVE model was parametrised so that CNTs interphase properties become input parameters. Whereas lamina elastic constants were output parameters. The optimisation study was performed with Multi-Objective Genetic Algorithm in ANSYS Design Explorer optimisation module. Transversely isotropic properties of the CNTs reinforced interphase were for the first time fully characterised inversely.

2. Numerical modelling of fuzzy fibre reinforced polymer

2.1. Fuzzy fibre reinforced polymer

Fig. 2a shows a schematic illustration of a single fuzzy fibre where CNTs are radially grown on the surface of carbon fibre. The fuzzy fibre consists of two distinct regions: a core fibre and the surrounding CNTs reinforced interphase. This interphase is composed of CNTs and epoxy resin and behaves transversely isotropic due to the unique orientation of CNTs. Local coordinates system 1′-2′-3′ is assigned to describe the CNTs reinforced interphase, where the 1′-axis is aligned with CNTs axial direction shown Fig. 2b. Fuzzy fibre is then embedded in epoxy resin, forming FFRP. The mechanical behaviour of FFRP material is effectively studied using hexagonal representative volume element (RVE) model, as depicted in Fig. 2c. In this numerical study of FFRP, fuzzy fibres are arranged in the unidirectional lamina and follow global coordinate system with axes denoted by 1–2-3, where the 1-axis is along the carbon fibre direction.

2.2. RVE model

The RVE model was implemented in ANSYS Design Parametric Language (APDL) module of ANSYS 19.0 software. The simulations in APDL can be executed entirely using commands; the commands collection file can be easily modified to maximise the operating efficiency of simulations. Motivated by experimental [1] and numerical studies [13], material selected for this study was T650/EPIKOTE 862 resin FRRP.

The RVE contained three phases: carbon fibre, the CNTs reinforced interphase and epoxy resin. The APDL script specified material properties of each phase, the geometry of RVE and boundary conditions. Mechanical and physical properties of transversely isotropic carbon fibre

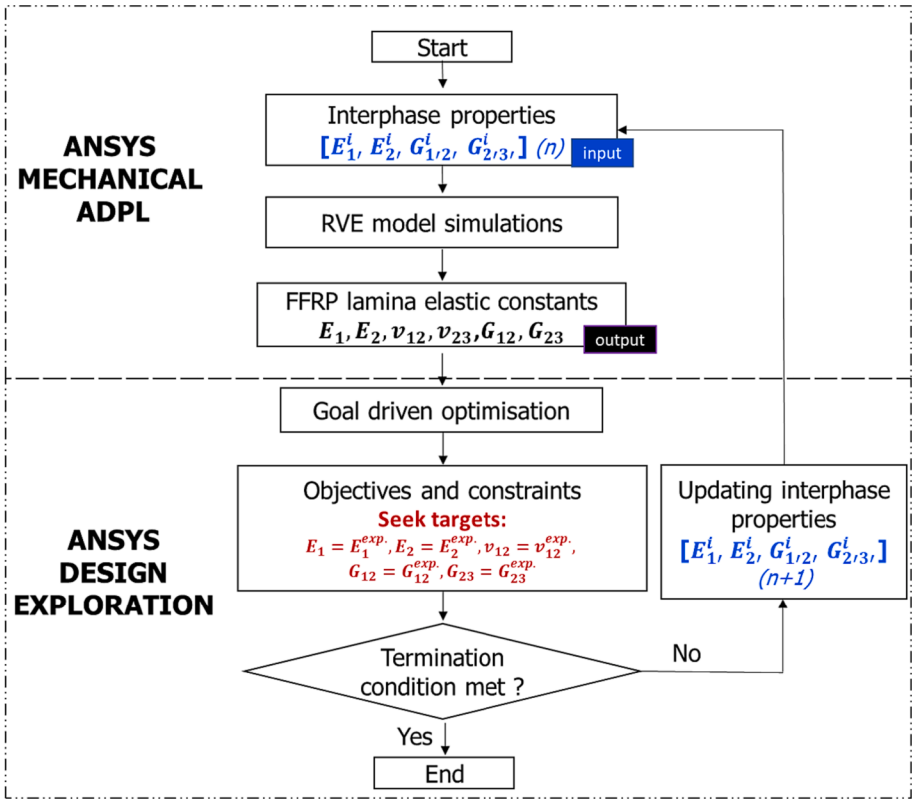

Fig. 3. Flow chart of optimisation procedure using ANSYS Workbench.

Table 2
Set of objectives interphase properties to satisfy in the optimisation study (adapted from [13]).

Fuzzy Fibre Lamina elastic constants (15 % carbon fibre volume fraction)	[13]
Longitudinal modulus, E_1 (GPa)	40.85
Transverse modulus, E_2 (GPa)	6.11
In-plane shear modulus, G_{12} (GPa)	2.07
Transverse shear modulus, G_{23} (GPa)	2.11
In-plane Poisson's ratio ν_{12} [a]	0.18
[a] predicted from RVE simulations	

Table 3
Upper and lower bounds of CNTs reinforced interphase properties.

CNTs reinforce interphase	**Lower bound**	**Upper bound**
Longitudinal modulus $E^i_{1'}$ (GPa)	200	400
Transverse modulus $E^i_{2'}$ (GPa)	1	10
In-plane shear modulus, $G^i_{1'2'}$ (GPa)	2	3
Transverse shear modulus, $G^i_{2'3'}$ (GPa)	2	3

Table 4
Objectives and constraints of the interphase parameters identification procedure.

Fuzzy Fibre Lamina elastic constants	Seek target[13]	Lower constraint (MOGA)	Upper constraint (MOGA)
Longitudinal modulus, E_1 (GPa)	40.85	40.80	40.90
Transverse modulus, E_2 (GPa)	6.11	6.10	6.12
In-plane shear modulus, G_{12} (GPa)	2.07	2.06	2.08
Transverse shear modulus, G_{23} (GPa)	2.11	2.10	2.12

and isotropic epoxy resin are given in Table 1 [13]. Dimensions of the RVE model were calculated based on the carbon fibre volume fraction and diameter. For 15 % of carbon fibre volume fraction, RVE's height, width and thickness were 6.15, 10.63 and 1.54 μm, respectively. The thickness of CNTs reinforced interphase was dictated by the length of CNTs and assumed as 2 μm [13]. The properties of CNTs reinforced interphase were adopted from [13] for the validation study of the RVE model. Perfect bonding conditions between each phase were assumed. The mesh type for the models adopted 20-node 3-D solid elements (SOLID186). Mesh independent test was accomplished to eliminate the influence of mesh density on the accuracy of the results. The whole meshed model contained approximately 7000 elements. The CNTs reinforced interphase was not isotropic; therefore, "VEORIENT" command was adopted to specify mesh element orientation for the meshed volume. The element orientation was determined by the one of the lines defining the RVE volume, namely the circumference of the carbon fibre. The normal direction of CNTs reinforced interphase elements (1' in local coordinates) followed the direction of the line, as shown in Fig. 1d [22].

The prediction of elastic constants of FFRP lamina was based on the Hooke's law for transversely isotropic materials. The periodic boundary conditions were applied to the RVE model to compute stresses and strains. The comprehensive description of the periodic boundary conditions used in this study can be found elsewhere [23,24]. Once simulations were completed, elastic constants of lamina can be calculated, including E_1 and E_2, the longitudinal and transverse moduli; ν_{12} and ν_{23}, the in-plane and out-of-plane Poisson's ratios; G_{12}, the in-plane shear modulus and G_{23}, the out-of-plane shear modulus. The validation of the present RVE model and the literature data was accomplished in our previous work [24]. Numerical results predicted by the hexagonal RVE perfectly matched analytical results calculated by the composite cylinder method [13].

3. Inverse method

3.1. CNTs reinforced interphase parameter identification procedure

This section presents the detailed procedure on how to predict the CNTs reinforced interphase properties using the combination of ANSYS Mechanical APDL and Design Exploration, as shown in Fig. 3. This application is integrated with ANSYS Workbench and allows parametric analyses to explore, understand and optimise the design conveniently. There are three types of the optimisation study in which objectives can be either *minimised*, *maximised* or *seek target*. The detailed guideline on how to implement optimisation in ANSYS Workbench is given by [25]. Firstly, the RVE model was parameterised, and random values were simulated to evaluate elastic constants of fuzzy fibre reinforced lamina using the ANSYS Mechanical APDL. Then, the identification process of CNTs reinforced interphase properties was performed with Goal-Driven Optimisation. The CNTs interphase properties were updated iteratively until the predicted lamina elastic constants matched the set of objective results. Objective results were adopted from the analytical study reported by [13]. This work provided a full set of FFRP lamina properties required for this exercise [1]. Full set of the properties of FFRP lamina can be experimentally tested and it is a common practice for composite manufactures to report lamina properties. Chatzigeorgiou et al. [13] studied the effects of different carbon fibre volume fraction on the elastic constants of FFRP lamina. The elastic constants of FFRP lamina (E_1;E_2; G_{12}; G_{23}) with 15 % carbon fibre volume fraction were extracted from the graph and selected as a set of objective results (see Table 2). The present method focused on the elastic properties of FFRP. The plastic properties and damage behaviour were out of the scope of this paper. Barbero et al. [25] used a similar approach to determine the damage of traditional laminated composites. This framework can also be further extended to the plastic behaviour and progressive damage of FFRP by revising the APDL command script and including damage initiation criteria.

3.2. Parameterisation of APDL script

The FEA analysis was controlled by an APDL script, which called for the evaluation of the elastic properties of the FFRP lamina. The CNTs reinforced interphase properties $(E^i_{1'}; E^i_{2'}; G^i_{1'2'}; G^i_{2'3'})$ has been parametrised the APDL script (see excerpt in Fig. A1, Appendix A). These properties were called *inputs* in ANSYS Design Explorer terminology [22]. Remaining material parameters, such as fibre diameter, RVE dimensions, interphase thickness, carbon fibre and matrix material properties were fixed. Transversely isotropic elastic properties of fuzzy fibre lamina $(E_1, E_2, \nu_{12}, G_{23}, G_{12})$, were selected as objective or called *outputs* in ANSYS.

3.3. Goal-Driven optimisation

In the next step, Goal Driven Optimisation was used to identify properties of CNTs reinforced interphase. Input parameters of the interphase were represented by $E^i_{1'}; E^i_{2'}; G^i_{1'2'}; G^i_{2'3'}$. The interphase material properties varied within the design space defined in Table 3. Upper and lower bounds of interphase input parameters were selected optionally, but within some reasonable range based on the literature [1,5,13]. Random values of four input parameters created one design point. The objective of this optimisation was to find the CNTs reinforced interphase properties so that the *outputs* $(E_1, E_2, \nu_{12}, G_{23}, G_{12})$ *seek target* of lamina properties, as shown in Table 4.

The goal-driven optimisation was performed with Multi-objective Genetic Algorithm (MOGA). MOGA is a variant of the popular non-dominated Sorted Genetic Algorithm-II (NSGA-II) based on controlled

Table 5
Properties of MOGA optimisation algorithm.

Method Name	MOGA
Estimated number of Design Points	1150
Number of Initial Samples	200
Number of Samples Per Iteration	50
Maximum Allowable Pareto Percentage	70
Convergence Stability Percentage	2
Maximum Number of Iterations	20
Maximum Number of Candidates	5

elitism concepts. This algorithm supports multiple objectives and constraints to find the global optimum. The settings of MOGA optimisation algorithm used in this study, are shown in Table 5. The iterative parameter identification process is repeated until the solution converges and candidate points (CNTs reinforced interphase properties) meet the required objectives and constraints. Firstly, the optimisation was run with the set objectives without constraints (see Table B1, Appendix B). To improve the accuracy of the analysis, upper and lower constraints on the objective were included in the optimisation, as shown in Table 4.

4. Results and discussion

4.1. History chart of output parameters of FFRP lamina

History charts of output parameters (fuzzy fibre lamina's elastic properties) were created for each design point for the interphase. Corresponding *seek target* value (objective of this study see Table 4) was included in the graph (dashed line). Fig. 4a presents the longitudinal modulus (E_1) of the fuzzy fibre lamina. Within the first 200 design points the E_1 varied widely between 38 GPa up to 47 GPa. Then, the evaluation of next generation design points brought the history chart of E_1 much closer to the seek target. After 400 design points, no significant variations from the target were observed. The transverse modulus (E_2) of the fuzzy fibre lamina versus the number of design points followed similar pattern to that of E_1. The initial 200 design points generated wild variation of E_2 in the range of 5.5 to 6.5 GPa. The next generation of interphase properties brought the output parameters closer to the target. After attempting around 500 design points, the E_2 value was found by satisfying the objective within a certain limit. The in-plane shear modulus (G_{12}) of the fuzzy fibre lamina varied from 1.9 GPa to 2.2 GPa. Evaluations of 500 design points caused G_{12} to fluctuate less. A small deviation of (0.15 GPa) between predicted final value and target remained in this optimisation. The out-of-plane lamina modulus (G_{23}) fluctuated from 1.8 GPa to 2.3 GPa with the initial design points data set. The seek target was met after testing more than 500 design points. The

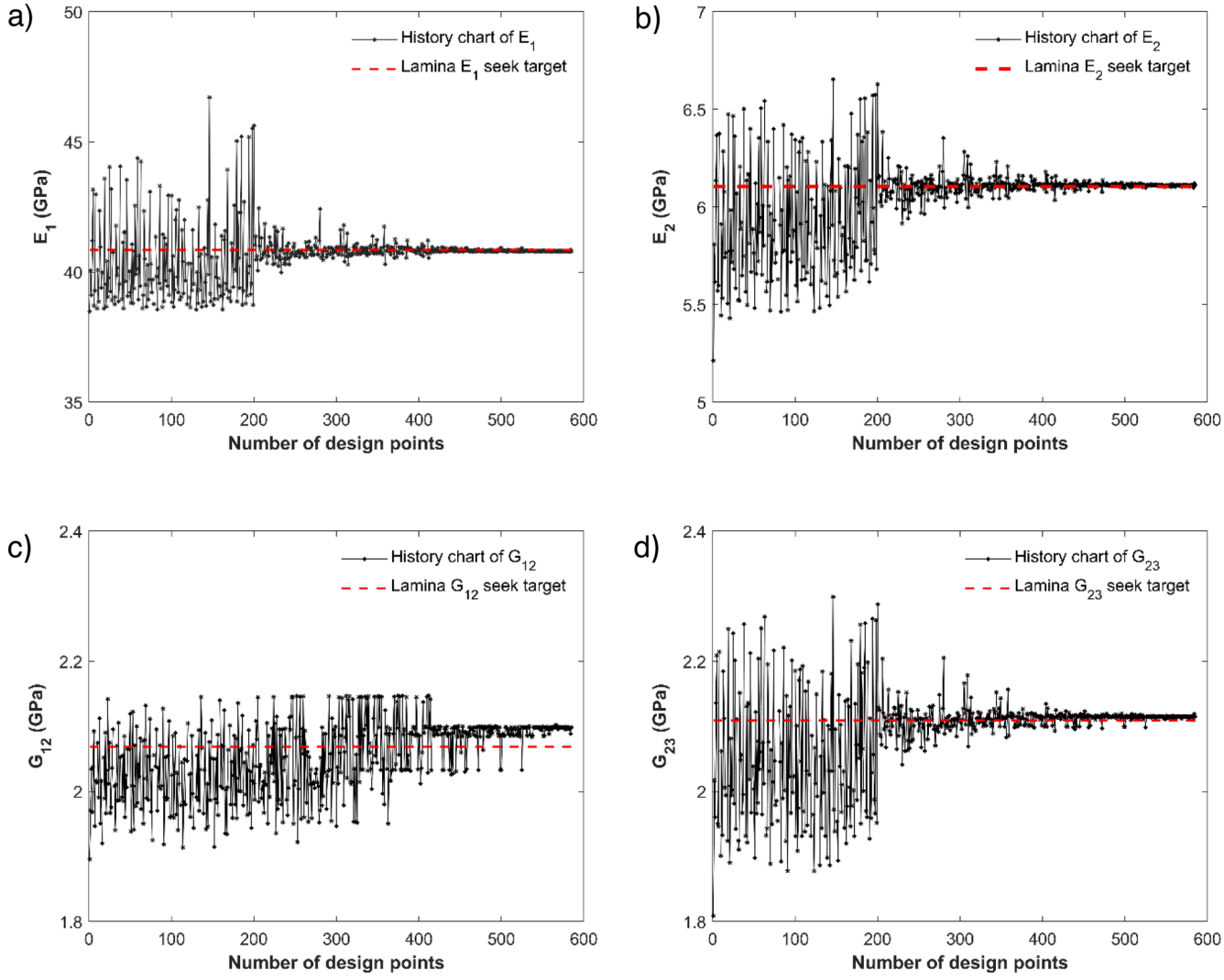

Fig. 4. History chart of output parameters namely elastic constants of FFRP lamina. Dashed line represents the seek target values.

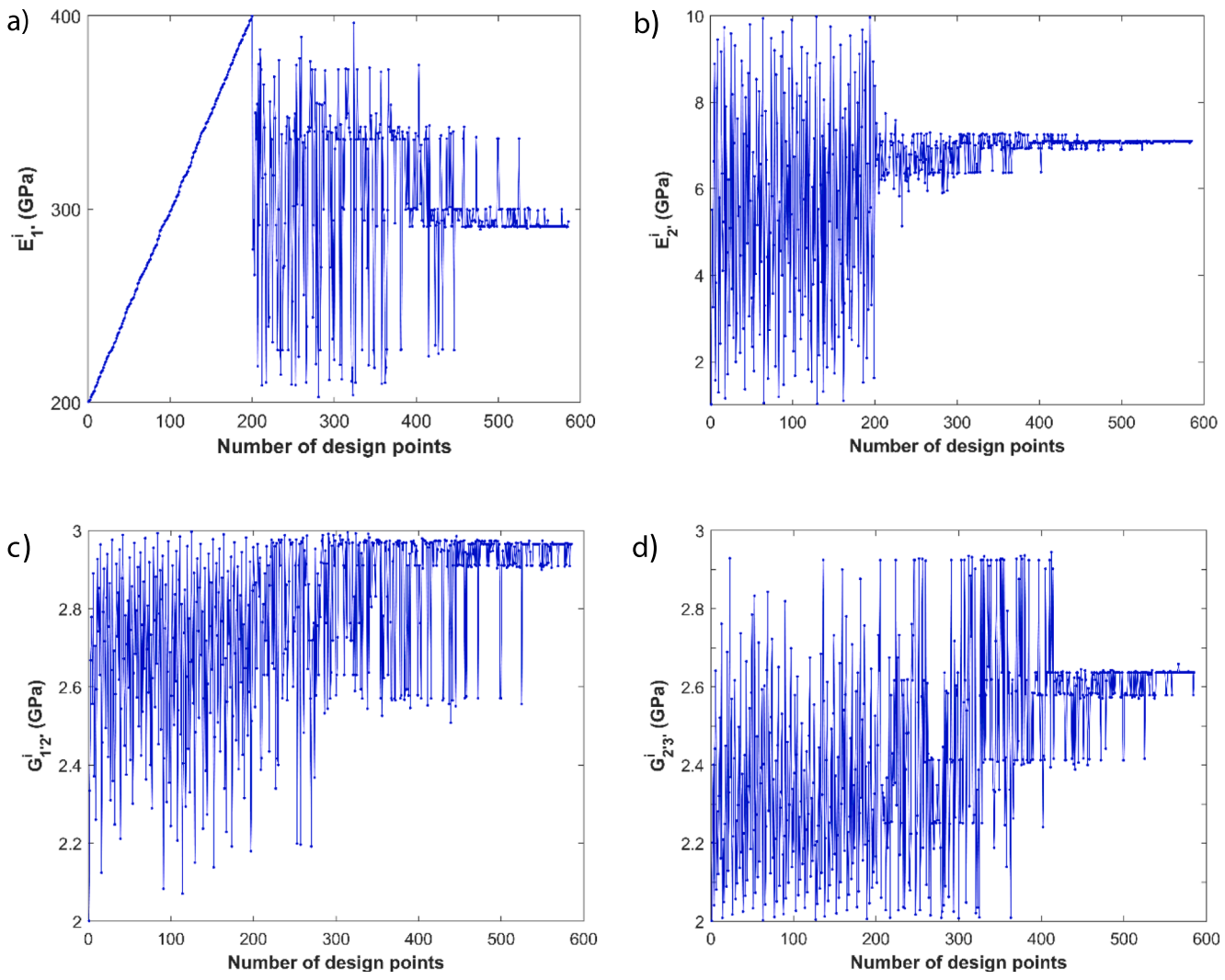

Fig. 5. History chart of the CNTs reinforced interphase input parameters.

Table 6
Candidate points of CNTs reinforced interphase properties identified from present optimisation procedure.

Properties	[13]	Candidate Point 1	Candidate Point 2	Candidate Point 3	Candidate Point 4	Candidate Point 5
E_1^i(GPa)	298.64	290.66	292.04	299.84	299.84	299.84
E_2^i(GPa)	7.01	7.06	7.11	7.09	7.09	7.09
G_{12}^i(GPa)	2.81	2.91	2.91	2.91	2.91	2.91
G_{23}^i(GPa)	2.52	2.58	2.64	2.64	2.64	2.64
E_1(GPa)	40.848	40.826	40.803	40.803	40.801	40.801
E_2(GPa)	6.105	6.109	6.105	6.109	6.109	6.109
G_{12}(GPa)	2.069	2.085	2.095	2.095	2.096	2.096
G_{23}(GPa)	2.109	2.113	2.112	2.112	2.112	2.112
ν_{12}	0.176	0.175	0.173	0.172	0.172	0.172

Table 7
Relative percentage error between the identified candidate points and CNTs reinforced properties from [13].

Properties	[13]	Candidate Point 1	Candidate Point 2	Candidate Point 3	Candidate Point 4	Candidate Point 5
E_1^i(GPa)	298.64	−2.7 %	−2.2 %	+0.4 %	+0.4 %	+0.4 %
E_2^i(GPa)	7.01	+0.7 %	+1.4 %	+1.1 %	+1.1 %	+1.1 %
G_{12}^i(GPa)	2.81	+3.6 %	+3.6 %	+3.6 %	+3.6 %	+3.6 %
G_{23}^i(GPa)	2.52	+2.3 %	+4.7 %	+4.7 %	+4.7 %	+4.7 %

```
/TITLE fuzzy fibre hexagonal RVE

rf=2.5          ! radius fibre in microns (μm)
a2=6.145        ! half of the width of RVE (μm)
a3=10.63        ! half of the height of RVE (μm)
a1=1.54         ! half of the thickness of RVE (μm)                    Fixed RVE dimensions

Ei1=298.64e-3   ! Longitudinal modulus of the interphase E1i, (TPa)
Ei2=7.01e-3     ! Transverse modulus of the interphase E2i, (TPa)
vi12=0.10       ! In-plane Poisson's ratio v12i,
vi23=0.39       ! Out-of-plane Poisson's ratio v23i,
Gi12=2.81e-3    ! In-plane shear modulus G12i, (TPa)
Gi23=2.52e-3    ! Out-of-plane shear modulus G23i, (TPa)               Parametrised properties of CNTs reinforced interphase

/prep7          ! Pre-processor module (Material properties)
MP,EX,1,14.50e-3   ! Transverse modulus of CF E2f (TPa)
MP,EY,1,14.50e-3   ! Transverse modulus of CF E2f (TPa)
MP,EZ,1,241.00e-3  ! Longitudinal modulus of CF E1f (TPa)
MP,nuXY,1,0.51     ! Transverse Poisson's ratio of CF v23f
MP,nuYZ,1,0.27     ! Longitudinal Poisson's ratio of CF v12f
MP,nuXZ,1,0.27     ! Longitudinal Poisson's ratio of CF v12f
MP,GXY,1,4.80e-3   ! Transverse Shear modulus of CF G23f (TPa)
MP,GYZ,1,22.80e-3  ! Longitudinal Shear modulus of CF G12f (TPa)
MP,GXZ,1,22.80e-3  ! Longitudinal Shear modulus of CF G12f (TPa)      Fixed Carbon Fibre properties
MP,EX,2,3.00e-3    ! Young's modulus of epoxy resin Em (TPa)
MP,PRXY,2,0.30     ! Poisson's ratio of epoxy resin νm                 Fixed Resin properties

MP,EX,3,Ei2
MP,EY,3,Ei2
MP,EZ,3,Ei1
MP,nuXY,3,(Ei2/(2*Gi23))-1
MP,nuYZ,3,0.1
MP,nuXZ,3,0.1
MP,GXY,3,Gi23
MP,GYZ,3,Gi12
MP,GXZ,3,Gi12                                                          INPUT PARAMETERS
```

Fig. A1. Parametrisation of CNTs reinforced interphase in APDL script file.

Table B1
Candidate points of the MOGA optimisation study without objective constraints.

	Experimental	Candidate Point 1	Candidate Point 2	Candidate Point 3
$E^i_{1'}$(GPa)	298.64	299.75	308.83	325.72
$E^i_{2'}$(GPa)	7.01	7.23	6.69	7.06
$G^i_{1'2'}$(GPa)	2.81	2.91	2.87	2.98
$G^i_{2'3'}$(GPa)	2.52	2.58	2.51	2.62
E_1(GPa)	40.848	40.956	40.637	40.806
E_2(GPa)	6.105	6.135	6.080	6.129
G_{12}(GPa)	2.069	2.085	2.070	2.096
G_{23}(GPa)	2.109	2.121	2.101	2.117
ν_{12}	0.176	0.178	0.170	0.171

computational time of evaluating 600 design points using the MOGA algorithm was approximately 5 h and 15 min on Intel Core i7-4770 K, 3.5 GHz, 16 GB RAM workstation.

4.2. History chart of input parameters of CNTs reinforced interphase

Fig. 5 shows how CNTs reinforced interphase parameters changes within the design space. MOGA evolves a population of individuals to find an optimal solution by attempting a number of design points. Initially, 200 design points were generated within the design space. Then, the next generations of design points (in the iteration of 50) were created based on the mutation of better fit individuals from the previous populations. After the evaluation of around 400 design points, the generated points started to converge. For example, the longitudinal ($E^i_{1'}$) and transverse ($E^i_{2'}$) moduli of the interphase fluctuated around 300 GPa and 7 GPa respectively. The design points of the in-plane shear modulus ($G^i_{1'2'}$) and out-of-plane shear modulus ($G^i_{2'3'}$) were around 2.9 GPa and 2.6 GPa, respectively. Convergence criteria (stability percentage) were met after evaluation of around 600 design points.

4.3. Predicted CNTs reinforced interphase properties (candidate points)

MOGA algorithm converged after 585 design points evaluations. Identified CNTs reinforced interphase properties were provided in the form of the five candidate points. The comparison of the identified candidate points and properties of the interphase [13] is shown in Table 6. The arithmetic percentage error between the predicted interphase properties and reference is shown in Table 7. Two candidate points (1 and 2) slightly underestimated the longitudinal interphase modulus ($E^i_{1'}$) with percentage error around 2 %. Remaining candidate points predicted well the $E^i_{1'}$ with an error smaller than 0.5 %. The transverse modulus of the interphase $E^i_{2'}$ was identified for all five candidate points with percentage error around 1 %. Slightly higher difference between identified shear moduli of the interphase was noticed (~5%). It is likely related to the lower sensitivity of the interphase shear moduli to the elastic constants of fuzzy fibre lamina. The average percentage error between predicted interphase properties and the one from [13] was around 2.5 %. It is possible that some accuracy was lost by rounding error.

4.4. Discussion

This inverse procedure was purposely designed to make full use of available experimental and numerical data, which demonstrated the key role of the CNTs reinforced interphase in FFRP. To consider the distinctive contribution from the CNTs reinforced interphase, a more

Table C1
Candidate points of CNTs reinforced interphase properties identified from present optimisation procedure (one input parameter, $E^i_{1'}$). Solution converged after 251 evaluations.

Properties	[13]	Candidate Point 1	Candidate Point 2	Candidate Point 3	Candidate Point 4	Candidate Point 5
$E^i_{1'}$(GPa)	298.64	298.79	297.83	296.5	296.5	295.5
E_1(GPa)	40.848	40.848	40.848	40.847	40.847	40.846
E_2(GPa)	6.105	6.105	6.104	6.103	6.103	6.103
G_{12}(GPa)	2.069	2.069	2.069	2.069	2.069	2.069
G_{23}(GPa)	2.109	2.109	2.109	2.109	2.109	2.109
ν_{12}	0.176	0.176	0.176	0.177	0.177	0.177

Table C2
Relative percentage error between the identified candidate point and CNTs reinforced properties from [13].

Properties	[13]	Candidate Point 1	Candidate Point 2	Candidate Point 3	Candidate Point 4	Candidate Point 5
$E^i_{1'}$(GPa)	298.64	+0.05 %	−0.27 %	−0.70 %	−0.70 %	+1.00 %

Table C3
Candidate points of CNTs reinforced interphase properties identified from present optimisation procedure (one input parameter, E_2^i). Solution converged after 351 evaluations.

Properties	[13]	Candidate Point 1	Candidate Point 2	Candidate Point 3	Candidate Point 4	Candidate Point 5
E_2^i(GPa)	7.01	7.009	7.011	7.009	7.008	7.008
E_1(GPa)	40.848	40.847	40.849	40.847	40.847	40.847
E_2(GPa)	6.105	6.105	6.104	6.103	6.103	6.103
G_{12}(GPa)	2.069	2.069	2.069	2.069	2.069	2.069
G_{23}(GPa)	2.109	2.109	2.109	2.109	2.109	2.109
ν_{12}	0.176	0.176	0.176	0.177	0.177	0.177

Table C4
Relative percentage error between the identified candidate point and CNTs reinforced properties from [13].

Properties	[13]	Candidate Point 1	Candidate Point 2	Candidate Point 3	Candidate Point 4	Candidate Point 5
E_2^i(GPa)	7.01	−0.01 %	+0.01 %	−0.01 %	−0.03 %	−0.03 %

Table C5
Candidate points of CNTs reinforced interphase properties identified from present optimisation procedure (one input parameter,$G_{1'2'}^i$). Solution converged after 283 evaluations.

Properties	[13]	Candidate Point 1	Candidate Point 2	Candidate Point 3	Candidate Point 4	Candidate Point 5
$G_{1'2'}^i$(GPa)	2.81	2.81	2.812	2.813	2.813	2.808
E_1(GPa)	40.848	40.848	40.848	40.848	40.848	40.848
E_2(GPa)	6.105	6.105	6.105	6.105	6.105	6.105
G_{12}(GPa)	2.069	2.069	2.069	2.069	2.069	2.069
G_{23}(GPa)	2.109	2.109	2.11	2.11	2.11	2.109
ν_{12}	0.176	0.176	0.176	0.177	0.177	0.177

Table C6
Relative percentage error between the identified candidate point and CNTs reinforced properties from [13].

Properties	[13]	Candidate Point 1	Candidate Point 2	Candidate Point 3	Candidate Point 4	Candidate Point 5
$G_{1'2'}^i$(GPa)	2.81	0.0 %	+0.07 %	+0.11 %	+0.11 %	−0.07 %

Table C7
Candidate points of CNTs reinforced interphase properties identified from present optimisation procedure (one input parameter,$G_{2'3'}^i$). Solution converged after 307 evaluations.

Properties	[13]	Candidate Point 1	Candidate Point 2	Candidate Point 3	Candidate Point 4	Candidate Point 5
$G_{2'3'}^i$(GPa)	2.52	2.519	2.522	2.523	2.523	2.523
E_1(GPa)	40.848	40.849	40.846	40.845	40.845	40.845
E_2(GPa)	6.105	6.105	6.104	6.104	6.104	6.104
G_{12}(GPa)	2.069	2.069	2.069	2.069	2.069	2.069
G_{23}(GPa)	2.109	2.1094	2.1093	2.1092	2.1092	2.1092
ν_{12}	0.176	0.176	0.176	0.177	0.177	0.177

Table C8
Relative percentage error between the identified candidate point and CNTs reinforced properties from [13].

Properties	[13]	Candidate Point 1	Candidate Point 2	Candidate Point 3	Candidate Point 4	Candidate Point 5
$G_{2'3'}^i$(GPa)	2.52	−0.04 %	+0.07 %	+0.11 %	+0.11 %	+0.11 %

advanced three-phase RVE model has to be used. In the FFRP, the unique radial orientation of CNTs grown on the carbon fibre causes the interphase to be transversely isotropic. Transversely isotropic features of the interphase complicated the RVE modelling. It increased the number of unknown parameters in the optimisation study to 4 from 2 for most commonly used isotropic features. Four elastic constants of CNTs reinforced interphase were predicted with the average percentage error around 2 % compared with true values. The high fidelity of inverse analysis results derived from conveniently implemented experimental data could be of singficant use in the future in characterising the difficult to measure interphase properties. To the best of the authors' knowledge, this is the first inverse parameters identification method to deal with the fuzzy fibre reinforced with transversely isotropic interphase.

Many studies investigated the CNTs reinforced interphase properties using analytical and numerical models [5,9–15]. Parametric studies revealed that interphase properties are greatly affected by CNTs distribution, waviness, length, diameter, volume fraction, CNT/matrix interfacial properties [15]. All above-mentioned models are useful in FFRP design; however, to simulate the full-scale laminate using these forward models, many input parameters of CNTs reinforced interphase

Table C9
Candidate points of CNTs reinforced interphase properties identified from present optimisation procedure (two input parameters $E^i_{1'}$, $E^i_{2'}$). Solution converged after 474 evaluations.

Properties	[13]	Candidate Point 1	Candidate Point 2	Candidate Point 3	Candidate Point 4	Candidate Point 5
$E^i_{1'}$(GPa)	298.64	300.95	301.28	301.72	301.68	301.68
$E^i_{2'}$(GPa)	7.01	7.002	7.002	7.002	7.001	7.001
E_1(GPa)	40.848	40.86	40.86	40.86	40.86	40.86
E_2(GPa)	6.105	6.101	6.100	6.101	6.101	6.101
G_{12}(GPa)	2.069	2.069	2.069	2.069	2.069	2.069
G_{23}(GPa)	2.109	2.11	2.11	2.11	2.11	2.11
ν_{12}	0.176	0.178	0.178	0.178	0.178	0.178

Table C10
Relative percentage error between the identified candidate points and CNTs reinforced properties from [13].

Properties	[13]	Candidate Point 1	Candidate Point 2	Candidate Point 3	Candidate Point 4	Candidate Point 5
$E^i_{1'}$(GPa)	298.64	+0.77 %	+0.88 %	+1.03 %	+1.02 %	+1.02 %
$E^i_{2'}$(GPa)	7.01	−0.11 %	−0.11 %	−0.11 %	−0.12 %	−0.12 %

Table C11
Candidate points of CNTs reinforced interphase properties identified from present optimisation procedure (two input parameters $G^i_{1'2'}$, $G^i_{2'3'}$). Solution converged after 510 evaluations.

Properties	[13]	Candidate Point 1	Candidate Point 2	Candidate Point 3	Candidate Point 4	Candidate Point 5
$G^i_{1'2'}$(GPa)	2.81	2.808	2.808	2.805	2.805	2.808
$G^i_{2'3'}$(GPa)	2.52	2.5198	2.5189	2.5197	2.5197	2.5197
E_1(GPa)	40.848	40.848	40.849	40.848	40.848	40.849
E_2(GPa)	6.105	6.1043	6.1045	6.104	6.104	6.1045
G_{12}(GPa)	2.069	2.0684	2.0683	2.0682	2.0682	2.0682
G_{23}(GPa)	2.109	2.109	2.109	2.109	2.109	2.109
ν_{12}	0.176	0.176	0.176	0.176	0.176	0.176

Table C12
Relative percentage error between the identified candidate points and CNTs reinforced properties from [13].

Properties	[13]	Candidate Point 1	Candidate Point 2	Candidate Point 3	Candidate Point 4	Candidate Point 5
$G^i_{1'2'}$(GPa)	2.81	−0.07 %	−0.07 %	−0.17 %	−0.17 %	−0.07 %
$G^i_{2'3'}$(GPa)	2.52	−0.01 %	−0.04 %	−0.01 %	−0.01 %	−0.01 %

are required. In a forward manner, material properties are predicted from a nanoscale (CNTs level), but parameters at nanoscale are not widely available (i.e., volume fraction, waviness). Quantitative characterisation of the interphase region remains a significant challenge. Experimental measurements of the nano-reinforced interphase properties are possible using nanoindentation, atomic force microscopy or dynamic mechanical mapping [19,20]. However, they are difficult due to size-scale effects [21]. So far, there are no direct experimental measurements of the FFRP's interphase elastic properties.

In this paper, the CNTs reinforced interphase properties were predicted from the lamina properties. It is widely accepted that lamina/laminate properties are much easier to be measured experimentally. The present procedure requires only one parameter of CNTs-reinforced interphase, namely thickness. However, this measurement is easier to be estimated experimentally, for example, using Scanning Electron Microscopy (see Fig. 1). Using the present method, the properties of the CNTs reinforced interphase are homogenised based on the thickness of the interphase region. This allows us to eliminate the unknown parameters i.e., CNTs waviness, length, diameter, volume fraction, CNT/matrix interfacial properties, needed in all forward numerical and analytical studies.

Inverse analysis and optimisation studies can be expensive in terms of computational time and suffer from non-unique solutions. From this study, it was identified that settings of the optimisation procedure in ANSYS Workbench affect the accuracy of the results. Optimisation without constraints on objectives converges faster, but the accuracy of the predicted interphase properties is reduced (Appendix B). Therefore, it is recommended to include constraints on objectives. The number of parameters to be determined also influences the accuracy and the uniqueness of the solutions. As shown in Appendix C, searching only one interphase parameter almost perfectly predicted the solution (Table C1-C12). Increasing the number of searched interphase parameters, slightly reduced the accuracy. This suggests some relationships between the parameters exist. To further improve the optimisation process, parameter sensitivity can be employed before defining the inverse problem. This sensitivity study could identify the weight and importance of interphase parameters on the FFRP lamina within the design space.

The advantage of the developed methodology is the utilisation of one software, which enables identifying parameters efficiently. This allows avoiding issues with coupling two software i.e., FEA package and optimisation algorithm. This type of parameter identification procedure gives the potential to predict the properties of any nano-engineered interphase. Nano-engineered interphase properties depend on the orientation of nanofillers in the interphase. The present model can be easily modified to accommodate not only transversely isotropic interphase, but also isotropic interphase. The transversely isotropic case corresponds to the more aligned distribution of nanofillers. While isotropic interphase in nano-engineered composites is present when nanoparticles are randomly orientated in the interphase [26]. These models are currently under development. Future studies will also focus

on the interphase parameter's identification from the laminate properties by coupling macro and microscale simulations. Knowing the homogenised interphase properties at microscale could further enable inversely predict the CNTs interphase characteristics at the nanoscale. For example, the geometrical features of the CNTs reinforced interphase, i.e., volume fraction or waviness, can be considered using the Mori Tanaka model [26,27]. This can be achieved by modifying the APDL commands script and incorporating the RVE made of CNTs and epoxy (Fig. 2a).

5. Conclusion

In this work, the problem of parameter identification of CNTs reinforced interphase of FFRP has been solved by the inverse strategy. The results are summarised as follows:

- Three-phase RVE model, in which interphase was transversely isotropic and CNTs radially grown on the carbon fibre surface, was developed to predict transversely isotropic properties of the FFRP lamina.
- Efficient parameter identification was achieved by a combination of Mechanical APDL and ANSYS DesignXplorer.
- The optimisation algorithm converged after 585 evaluations. Five potential candidate points which meet required objective and constrained were found. The identified interphase properties agreed well with the literature with an average percentage error of around 2 %.
- The influence of settings in the optimisation procedure on the accuracy of the results was critically discussed.
- The accurate prediction proves the effectiveness of employing the proposed parameter identified procedure to obtain mechanical properties of nano-reinforced interphase, which are difficult to measure experimentally.

D ata availability

The raw/processed data (APDL code) required to reproduce these findings are available to download from [28].

CRediT authorship contribution statement

Marzena Pawlik: Conceptualization, Methodology, Software, Formal analysis, Writing – original draft. **Huirong Le:** Writing – review & editing, Supervision. **Paul Wood:** Writing – review & editing, Supervision. **Yiling Lu:** Conceptualization, Methodology, Formal analysis, Investigation, Writing – review & editing.

Declaration of Competing Interest

The authors declare that they have no known competing financial interests or personal relationships that could have appeared to influence the work reported in this paper.

Data availability

I have shared the APDL code through Mendeley repository and cited in the Reference List

Acknowledgement

This work was supported by School of Computing and Engineering, College of Science and Engineering, University of Derby, Markeaton Street, Derby, DE22 3AW, UK.

Appendix A

Appendix A presents the parametrisation of CNTs reinforced interphase parameters in the APDL script file.

Appendix B

Appendix B presents the results of parameter identification procedure without objective contraints.

Appendix C

Appendix C presents the parameters identification procedure by varying the number of input properties of the interphase. This helps to observe how each parameters effects the accuracy and solution convergence.

References

[1] R.J. Sager, P.J. Klein, D.C. Lagoudas, Q. Zhang, J. Liu, L. Dai, et al., Effect of carbon nanotubes on the interfacial shear strength of T650 carbon fiber in an epoxy matrix, Compos. Sci. Technol. 69 (2009) 898–904, https://doi.org/10.1016/j.compscitech.2008.12.021.

[2] C.D. Wood, M.J. Palmeri, K.W. Putz, G. Ho, R. Barto, B.L. Catherine, Nanoscale structure and local mechanical properties of fiber-reinforced composites containing MWCNT-grafted hybrid glass fibers, Compos. Sci. Technol. 72 (2012) 1705–1710, https://doi.org/10.1016/j.compscitech.2012.06.008.

[3] S.Y. Jin, R.J. Young, S.J. Eichhorn, Hybrid carbon fibre-carbon nanotube composite interfaces, Compos. Sci. Technol. 95 (2014) 114–120, https://doi.org/10.1016/j.compscitech.2014.02.015.

[4] Z.-G. Zhao, L.-J. Ci, H.-M. Cheng, J.-B. Bai, The growth of multi-walled carbon nanotubes with different morphologies on carbon fibers, Carbon N Y 43 (2005) 663–665, https://doi.org/10.1016/j.carbon.2004.10.013.

[5] M. Kulkarni, D. Carnahan, K. Kulkarni, D. Qian, J.L. Abot, Elastic response of a carbon nanotube fiber reinforced polymeric composite: A numerical and experimental study, Compos. B Eng. 41 (2010) 414–421, https://doi.org/10.1016/j.compositesb.2009.09.003.

[6] E.T. Thostenson, W.Z. Li, D.Z. Wang, Z.F. Ren, T.W. Chou, Carbon nanotube/carbon fiber hybrid multiscale composites, J. Appl. Phys. 91 (2002) 6034–6037, https://doi.org/10.1063/1.1466880.

[7] R.B. Mathur, S. Chatterjee, B.P. Singh, Growth of carbon nanotubes on carbon fibre substrates to produce hybrid/phenolic composites with improved mechanical properties, Compos. Sci. Technol. 68 (2008) 1608–1615, https://doi.org/10.1016/j.compscitech.2008.02.020.

[8] J. Karger-Kocsis, H. Mahmood, A. Pegoretti, All-carbon multi-scale and hierarchical fibers and related structural composites: A review, Compos. Sci. Technol. 186 (2019) 107932, https://doi.org/10.1016/J.COMPSCITECH.2019.107932.

[9] S.I. Kundalwal, M.C. Ray, Micromechanical analysis of fuzzy fiber reinforced composites, Int. J. Mech. Mater. Des. 7 (2011) 149–166, https://doi.org/10.1007/s10999-011-9156-4.

[10] S.I. Kundalwal, M.C. Ray, Effective properties of a novel continuous fuzzy-fiber reinforced composite using the method of cells and the finite element method, Eur J Mech - A/solids 36 (2012) 191–203, https://doi.org/10.1016/j.euromechsol.2012.03.006.

[11] R. Rafiee, A. Ghorbanhosseini, Stochastic multi-scale modeling of randomly grown CNTs on carbon fiber, Mech. Mater. 106 (2017) 1–7, https://doi.org/10.1016/j.mechmat.2017.01.001.

[12] S.I. Kundalwal, M.C. Ray, Effect of carbon nanotube waviness on the effective thermoelastic properties of a novel continuous fuzzy fiber reinforced composite, Compos. B Eng. 57 (2014) 199–209, https://doi.org/10.1016/j.compositesb.2013.10.003.

[13] G. Chatzigeorgiou, G.D. Seidel, D.C. Lagoudas, Effective mechanical properties of "fuzzy fiber" composites, Compos. B Eng. 43 (2012) 2577–2593, https://doi.org/10.1016/j.compositesb.2012.03.001.

[14] Y. Rao, J. Ban, S. Yao, K. Wang, N. Wei, Y. Lu, et al., A hierarchical prediction scheme for effective properties of fuzzy fiber reinforced composites with two-scale interphases: Based on three-phase bridging model, Mech. Mater. 152 (2021) 103653, https://doi.org/10.1016/j.mechmat.2020.103653.

[15] M.K. Hassanzadeh-Aghdam, R. Ansari, A. Darvizeh, Micromechanical analysis of carbon nanotube-coated fiber-reinforced hybrid composites, Int. J. Eng. Sci. 130 (2018) 215–229, https://doi.org/10.1016/j.ijengsci.2018.06.001.

[16] H.W. Wang, H.W. Zhou, R.D. Peng, L. Mishnaevsky, Nanoreinforced polymer composites: 3D FEM modeling with effective interface concept, Compos. Sci. Technol. 71 (2011) 980–988, https://doi.org/10.1016/j.compscitech.2011.03.003.

[17] J. Lu, P. Zhu, Q. Ji, Q. Feng, J. He, Identification of the mechanical properties of the carbon fiber and the interphase region based on computational micromechanics and Kriging metamodel, Comput. Mater. Sci 95 (2014) 172–180, https://doi.org/10.1016/j.commatsci.2014.07.034.

[18] A. Matzenmiller, S. Gerlach, Parameter identification of elastic interphase properties in fiber composites, Compos. B Eng. 37 (2005) 117–126, https://doi.org/10.1016/j.compositesb.2005.08.003.

[19] A. Matzenmiller, S. Gerlach, Parameter identification of elastic interphase properties in fiber composites, Compos. B Eng. 37 (2005) 117–126, https://doi.org/10.1016/j.compositesb.2005.08.003.

[20] R. Rafiee, A. Ghorbanhosseini, Stochastic multi-scale modeling of randomly grown CNTs on carbon fiber, Mech. Mater. 106 (2017) 1–7, https://doi.org/10.1016/j.mechmat.2017.01.001.
[21] X. Ren, J. Burton, G.D. Seidel, K. Lafdi, Computational multiscale modeling and characterization of piezoresistivity in fuzzy fiber reinforced polymer composites, Int. J. Solids Struct. 54 (2015) 121–134, https://doi.org/10.1016/j.ijsolstr.2014.10.034.
[22] ANSYS. ANSYS 2018. www.ansys.com (accessed March 30, 2021).
[23] E.J. Barbero, Finite Element Analysis of Composite Materials Using ANSYS, CRC Press, Second, 2014.
[24] M. Pawlik, Y. Lu, Prediction of elastic constants of the fuzzy fibre reinforced polymer using computational micromechanics.IOP Conf, Ser.: Mater. Sci. Eng. 362 (2018), 012006, https://doi.org/10.1088/1757-899X/362/1/012006.
[25] E.J. Barbero, M. Shahbazi, Determination of material properties for ANSYS progressive damage analysis of laminated composites, Compos. Struct. 176 (2017) 768–779, https://doi.org/10.1016/j.compstruct.2017.05.074.
[26] M. Pawlik, H. Le, Y. Lu, Effects of the graphene nanoplatelets reinforced interphase on mechanical properties of carbon fibre reinforced polymer – A multiscale modelling study, Compos. B Eng. (2019) 177, https://doi.org/10.1016/j.compositesb.2019.107097.
[27] B. Adhikari, B.N. Singh, A Coupled Mori-Tanaka model and FEM RVE approach for the geometrical nonlinear dynamic response of the FG-CNTRC plate based on a novel shear strain function using isogeometric finite element procedure, Compos. Struct. 280 (2022) 114947, https://doi.org/10.1016/j.compstruct.2021.114947.
[28] M. Pawlik, APDL command collection file, Mendeley Data V1 (2023), https://doi.org/10.17632/g53d8wc9d2.1.